Journal of Structural Geology, Vol. 14, No. 5, pp. 521 to 530, 1992
Printed in Great Britain

0191-8141/92 $05.00+0.00

Stress field and thrust kinematics: a model for the tectonic inversion of the Cameros Massif (Spain)

ANTONIO M. CASAS-SAINZ and JOSÉ L. SIMÓN-GÓMEZ

Departamento de Geología, Universidad de Zaragoza, 50009 Zaragoza, Spain

(*Received* 18 *March* 1991; *accepted in revised form* 10 *December* 1991)

Abstract—Alpine tectonics of the Cameros Thrust has been studied from several points of view: geometry (surface and sub-surface structure, three-dimensional outline of the thrust), kinematics (transport direction) and dynamics (characterization of the regional compressional stress field). All three aspects are related by means of a model based on Bott's equation. Under a N to NNE horizontal compression, with an average stress ratio $R = (\sigma_z - \sigma_x)/(\sigma_y - \sigma_x) = 0.2$, the eastern ramp of the Cameros Thrust (oriented 155°, 30°W) underwent a strike-slip right-lateral movement with a small reverse component. This gave rise to rigid displacement of the Cameros block towards the NNW and produced a 'guided movement' on the western, frontal ramp (oriented 060°, 13°S).

INTRODUCTION

THE Cameros Massif, together with the Sierra de la Demanda, forms the north-westernmost sector of the Iberian Chain. This is an intraplate chain built up mainly during the Palaeogene between the Ebro, Duero and Tajo Tertiary basins. The Cameros Massif is made up of a thick cover of Jurassic and Cretaceous rocks overlying the Hercynian basement and the Triassic of Germanic facies, the clay and gypsum beds of the Keuper acting as a detachment level between both structural levels. The region shows a structure of flat lying beds only disturbed by some gentle folds trending E–W and NW–SE (Fig. 1).

To the north of the Cameros Massif is the western sector of the Ebro Basin, filled with Tertiary continental clastic, lutitic and evaporitic deposits (4000–5000 m thick). The boundary between these two units is an important thrust with a large horizontal displacement, 25–30 km after Casas-Sainz (1990) and 30–35 km after Guimerà & Alvaro (1990). The strike of this thrust changes from NE–SW in the western part to E–W and NW–SE in the east, forming a continuous front of 90 km.

Westwards of the Cameros Massif, the Hercynian basement of the Sierra de la Demanda overthrusts the Tertiary deposits of the Ebro Basin. The strike of this new thrust is slightly different from that of the western part of the Cameros Thrust (see the Anguiano area on the maps of Figs. 1 and 3). The contact between the Demanda and the Cameros massifs shows compressive structures, which have been interpreted as related to a lateral ramp uplifting the Hercynian basement over the Mesozoic rocks of the Cameros Basin (Ramírez *et al.* in press). This implies a relative convergent movement between these two massifs within the hanging wall of the whole thrust sheet, and some independence of their respective displacement vectors.

The different directions of the thrust front are strongly conditioned by basement faults whose vertical displacement during the Upper Jurassic–Lower Cretaceous gave rise to the development of the Cameros Basin. This has been interpreted as a synclinal basin developed over a half-graben within the basement, the latter being controlled by NW–SE normal faults in its NE boundary. Jurassic limestones were detached over Upper Triassic plastic beds and stretched without losing their overall continuity, and covered by 5000 m of fluvial and lacustrine deposits (Guiraud & Séguret 1984). During the Tertiary, the listric normal faults which controlled the development and subsidence of the graben moved with a reverse component, in a process of *tectonic inversion* which recovered the former normal offset and raised the Cameros block to its present position (see Figs. 2b&c). Thus, the present thrust delimits more or less the northern margin of the Cretaceous basin, and the geometry of the thrust surface below the Cameros massif constitutes an accurate replica of it.

The Cretaceous sequence has been well preserved during the Tertiary compressional stage (Tischer 1966, Guiraud & Séguret 1984). The Cameros Massif moved as a solid block, undergoing internal deformations of very small amplitude relative to the throw of the thrust; the gentle E–W and NW–SE folds mentioned above, which constitute the most important structures in the interior of the massif, are considered to be of Cretaceous age. That was possible because of (1) the presence of the Keuper detachment level, and (2) the rigid behaviour of the thick Cretaceous sequence, in part due to the hardening caused by diagenesis and incipient metamorphism during the Lower Cretaceous (Guiraud & Séguret 1984).

Thrusting occurred in the Tertiary under a nearly N–S compressional field by propagation through the northern part of the Iberian plate from its convergent margin with the European plate. Characterization of this stress field has been possible by using palaeostress analysis from fault populations measured in a number of selected outcrops.

The purpose of the present work is to integrate vari-

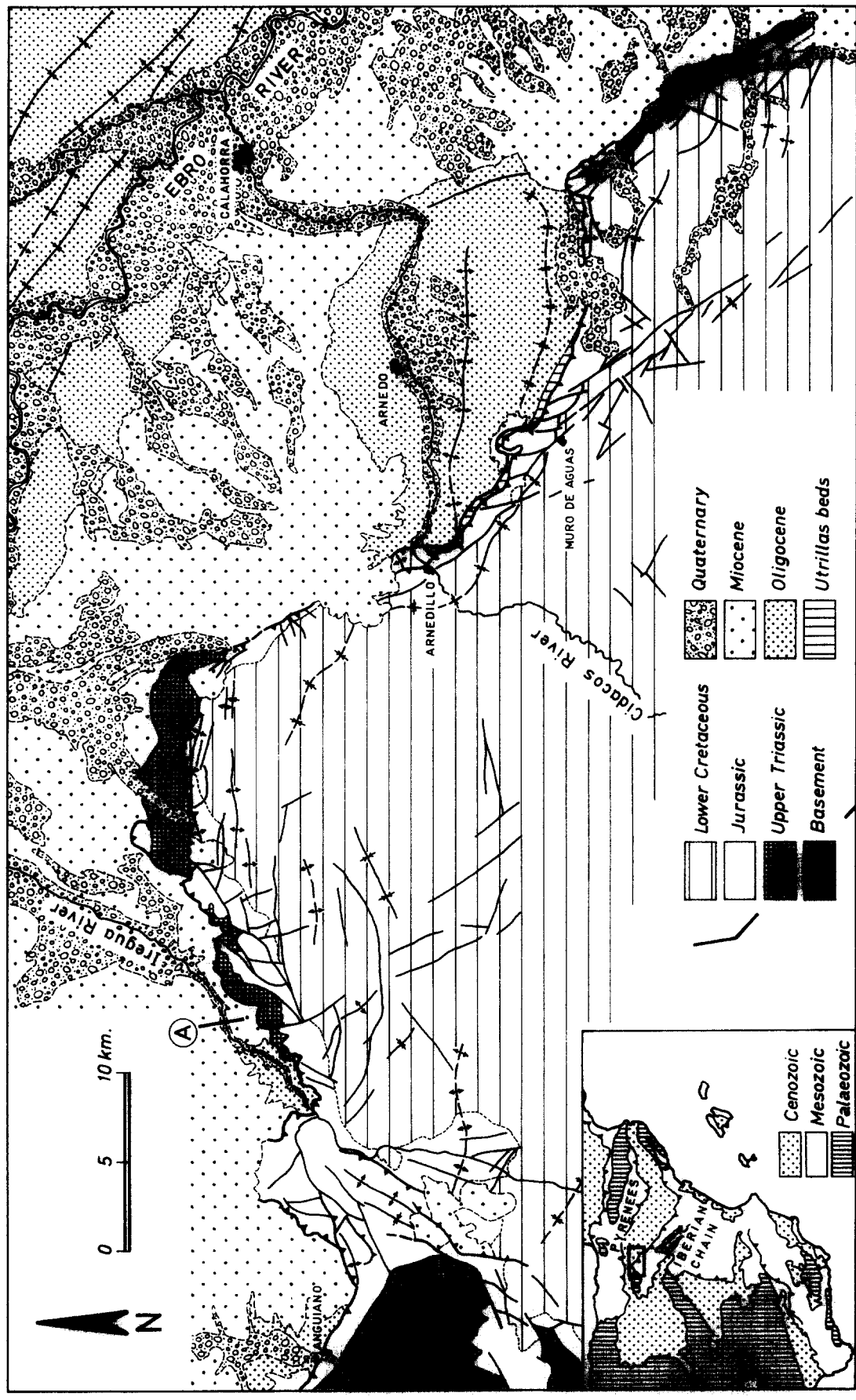

Fig. 1. Structural map of the northern front of the Cameros Massif and location of the area within the Iberian Peninsula. A–B shows the position of the cross-section in Fig. 2.

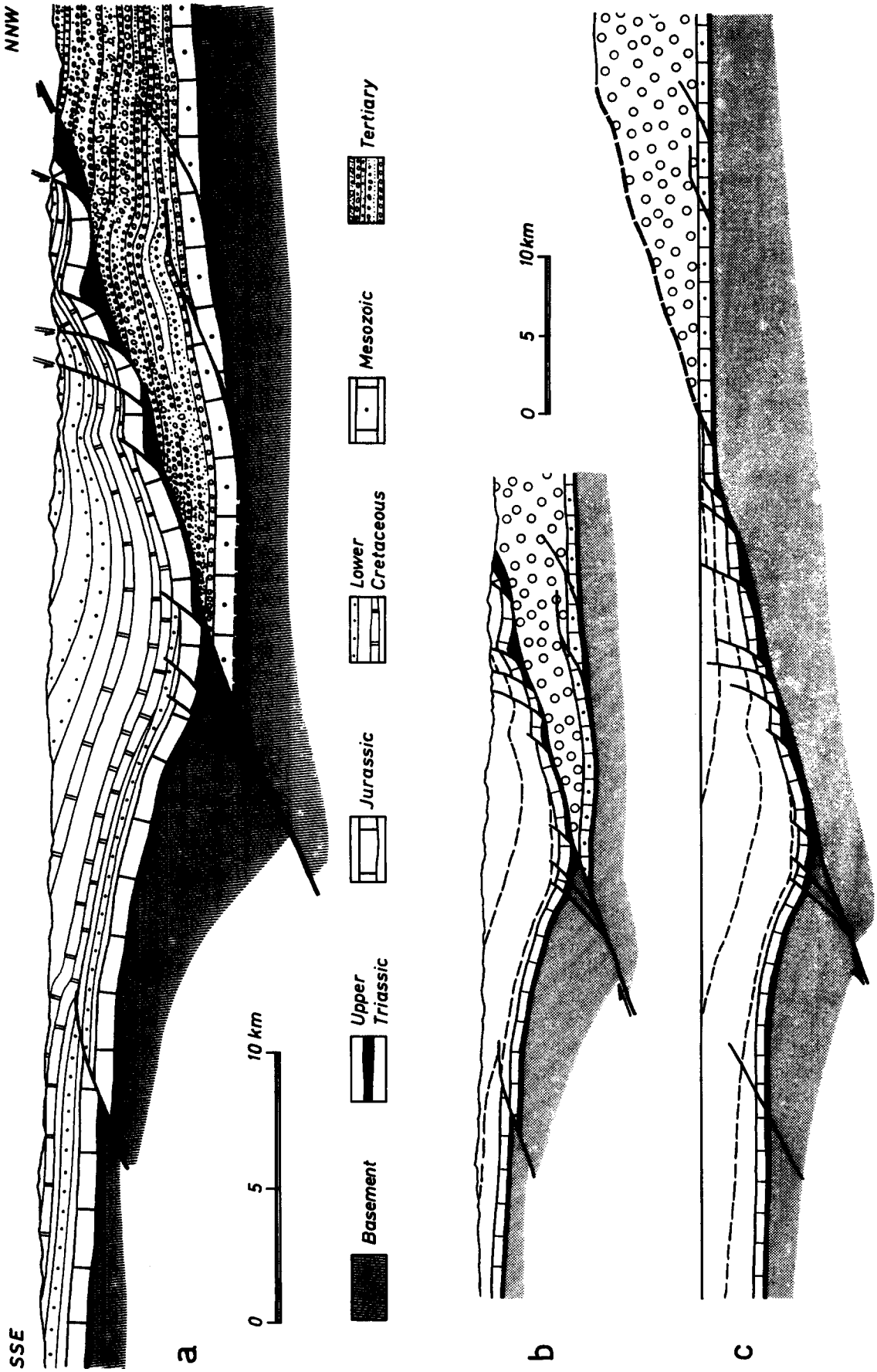

Fig. 2. (a) Structural section along the Cameros Massif (see A–B in Fig. 1). (b) Reduced sketch. (c) Restored section showing the original structure of the Cameros Basin; this one cannot be sequentially restored because it is oblique to the extension direction.

ous types of information (geometry, transport direction and stress field), obtained from completely independent methods and reported in the following sections, into a kinematic–dynamic model based on Bott's equation (Bott 1959):

$$\tan \theta = (n/lm)\,[m^2-(1-n^2)\,(\sigma_z-\sigma_x/(\sigma_y-\sigma_x)],$$

where θ is the pitch of the potential slip vector on the fault plane (parallel to the shear component); l, m, n are the direction cosines of the fault plane referred to the principal stress axes; and σ_x, σ_y and σ_z are the principal stresses so that σ_z is vertical or near vertical and $\sigma_y > \sigma_x$. From this model it will be demonstrated how the external stress field, acting on fault planes of known geometry, has determined the type and orientation of the thrust movement inferred from field data.

In our opinion, the use of Bott's equation is justified in this case for several reasons.

(1) Thrusting occurred inside the Iberian plate, so that faulting was not directly controlled by the kinematics of the northern, nearest plate margin but by the stress field propagated from that margin through the northern Iberian Peninsula.

(2) As we will see later, our stress analysis allows us to define approximately the mean features of the external stress field, so that they can be introduced into the calculations as simple numbers expressing the average axis orientation and stress ratio.

(3) The rigid behaviour of the Cameros block, with Tertiary deformation scarce and mainly restricted to its boundaries, approaches the conditions needed for solving the problem by means of brittle failure analysis.

THREE-DIMENSIONAL GEOMETRY OF THE THRUST SURFACE

Macrostructures of the Cameros region have been recently studied by Casas-Sainz (1990). Using detailed mapping of surface structures as well as subsurface data (deep boreholes and seismic profiles), several structural sections across the massif have been made (Fig. 2). Almost all of them show a single low-angle thrust, except those in the eastern zone (Arnedo). Here two thrust surfaces can be differentiated: an older (Oligocene–Lower Miocene) blind thrust whose surface expression is the ramp-induced anticline of Arnedo and a younger one (Middle–Upper(?) Miocene) which moved over the former structure and constitutes the present Mesozoic–Tertiary boundary at the surface.

By integrating data from all the structural sections, a contour map of the thrust surface can be constructed which represents its three-dimensional geometry (Fig. 3a). The map shows a zone of maximum dip of the surface (about 30°) below the eastern sector of the thrust front (oriented SSE), and another zone with average dip of 13° below the western sector (oriented ENE). Between both there exists an area where the thrust surface lies nearly horizontal. This geometry can be considered, for the purpose of the model, as being composed of two ramps striking nearly orthogonal to each other (average orientations of 155°/30°W and 060°/13°S) and a flat (Fig. 3b).

THE DIRECTION OF TECTONIC TRANSPORT. KINEMATIC INDICATORS

A number of kinematic indicators have been observed along the thrust front, either on or near the thrust surface. Almost all of them are in good agreement with a single movement towards the NNW, so that a transport of the whole Cameros block in this direction can be seen as a reasonable hypothesis.

The arguments that support this interpretation are the following (Fig. 4).

(1) Many striations measured on the thrust surface in the western sector have an average azimuth of 340–345°.

(2) Associated with the eastern ramp we have observed a secondary hangingwall thrust, parallel to the main one, showing strike-slip striations. In this sector there are also some folds trending ENE.

(3) The Arnedo anticline (see Fig. 4) seems to represent a 'compressional step' between two different segments of the eastern ramp. This also agrees with a main strike-slip movement on this ramp.

Therefore the western sector of the thrust (striking ENE) can be considered as a frontal ramp, whereas the eastern one (SSE) represents an oblique, nearly lateral ramp (showing only a minor reverse component). If we consider the striations measured in the western sector as the most reliable data, the azimuth of the average displacement vector for the whole Cameros block can be estimated as being 340–345°. That means that the tectonic inversion was not coaxial: the Tertiary thrusting took place following a transport direction at about 60° from the NE–SW Cretaceous extension.

THE REGIONAL STRESS FIELD

Palaeostresses related to the Tertiary compressional period have been inferred from stylolites and striated fault planes measured in 25 outcrops. Unfortunately, although a search for mesostructural sites was made over the entire region during a 4-year field survey, due to the lack of suitable rocks the sites are not homogeneously distributed but concentrated near the thrust front both in marine Jurassic limestones and Oligocene and Miocene conglomerates. Striation analysis has been made by combining three methods: right dihedra (Angelier & Mechler 1977), Etchecopar's method (Etchecopar *et al.* 1981) and y–R diagram (Simón-Gómez 1986). From this analysis we have obtained, at each site, both the orientation and shape of the deviatoric stress ellipsoid, the latter being represented by the stress ratio used in Bott's equation: $R = (\sigma_z-\sigma_x)/(\sigma_y-\sigma_x)$. This study makes an essential part of the Ph.D. thesis of Casas-Sainz (1990), and is exposed in more detail in Casas *et al.* (in press).

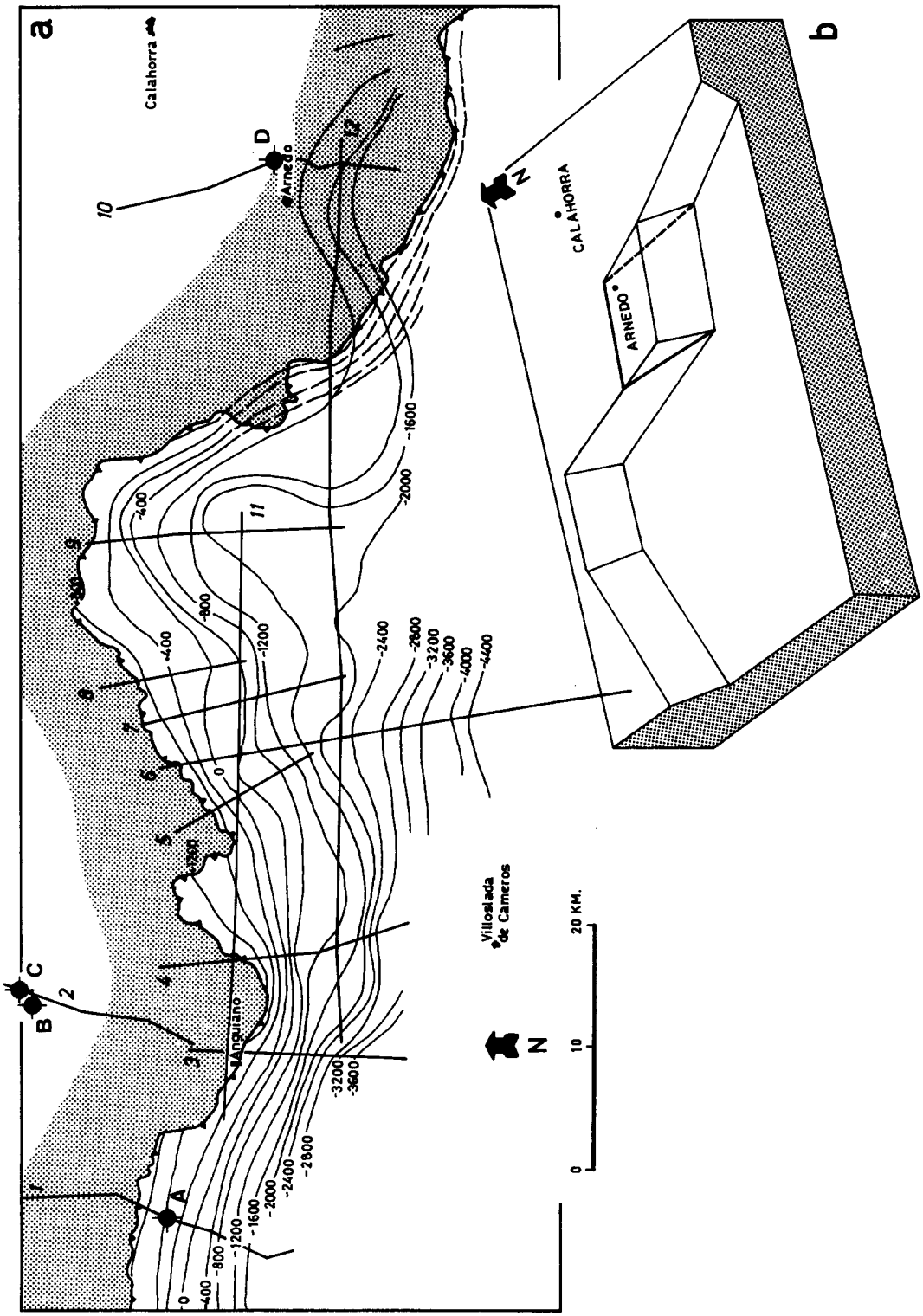

Fig. 3. (a) Contour map of the Cameros thrust surface, elaborated from seismic profiles (1, 2, etc.) and borehole information (A, B, etc.). Heights are expressed in metres above mean sea level. In the eastern zone two different surfaces are distinguished: a lower, blind thrust (continuous isolines) and an upper one (discontinuous isolines). (b) Three-dimensional outline showing the pattern of thrust ramps simplified from the contour map.

All the results are compiled in the synthetic y–R diagram of Fig. 5(a), without taking into account the plunge of the stress axes (y = azimuth of σ_y, R = stress ratio; $\sigma_y = \sigma_1$ if $R < 1$, $\sigma_y = \sigma_2$ if $R > 1$). A wide range of σ_1 directions can be seen, although most of them are oriented around N–S (between 150° and 025°). On the other hand, if we take into account the number of faults used for defining each ellipsoid (see rose diagram of Fig. 5b) we find that the directions between 000 and 020° are clearly the most frequent.

Consider now the spatial distribution of stress (Fig. 5c). The 000–020° compression is the most common in the analyzed stations, whereas the NNW one is present only in the western sector and, more clearly, in a zone situated to the south of Arnedo and limited by two broad fault zones running NNW–SSE: the thrust front and the Muro de Aguas fault zone. These facts suggest that the 000–020° compression represents the true 'primary' or external stress field, whereas the other directions represent local deflections of the former induced by major structures. In the case of the Arnedo zone, the observed type of deflection can be easily explained (according to the models of Xiaohan 1983) as a consequence of its location within the compressional step between the eastern right-lateral faults.

The hypothesis of a single stress field has received further support after performing a mathematical model using the finite element method (Casas-Sainz 1990, Casas *et al.* in press). According to this model most of the stress directions inferred from field data can be explained by a single NNE horizontal compression deflected by some major discontinuities. On the other hand, some data obtained within the Ebro Basin, where no major fault seems to be active under the mentioned compressional field, show only N to NNE compression (Gracia & Simón 1986, Casas-Sainz 1990). The same regional compression direction has been inferred in neighbouring areas (i.e. the linking zone between the Iberian Chain and Catalan Coastal Ranges) from geometry and kinematics of macrostructures (Guimerà 1984, 1988).

The alternative hypothesis of a primary compression oriented NNW (parallel to the second maximum in the diagram of Fig. 5b and normal to the western ramp) has been laid aside. The stress tensors showing NNE σ_1 axes could not be explained as local deflections of a NNW compression according to the model of Xiaohan (1983). So a NNW compression cannot be the only primary field in the region. It is true that the NNW compressional field, which represents the main Miocene compression direction in the eastern part of the Iberian Chain (Simón-Gómez 1986) could act beside the NNE one. Nevertheless, it is unlikely since no firm evidence of it has been found in our region; all the NNW σ_1 directions obtained are located in areas showing major faults able to produce deflections of stress trajectories which are well explained by our regional stress model.

Briefly, the regional or 'primary' stress field responsible for the thrust movement of the Cameros block can be characterized using only a part of the y–R diagram of Fig. 5(a) (marked with a rectangle). The σ_1 direction ranges from 000° to 025° (mean 012°) and the stress ratio is between 0.5 and −0.1 (mean 0.2).

RELATIONSHIP BETWEEN THRUST MOVEMENT AND REGIONAL STRESS FIELD

Can the thrust movement be explained by the stress field inferred using Bott's equation? To answer this question we analyse separately the movement on each ramp of the Cameros Thrust. We start with the eastern, nearly lateral ramp, by applying Bott's equation to the average values of the stress field and ramp orientation. The results are plotted on Fig. 6 (pitch of striation against R ratio). The central diagram shows the

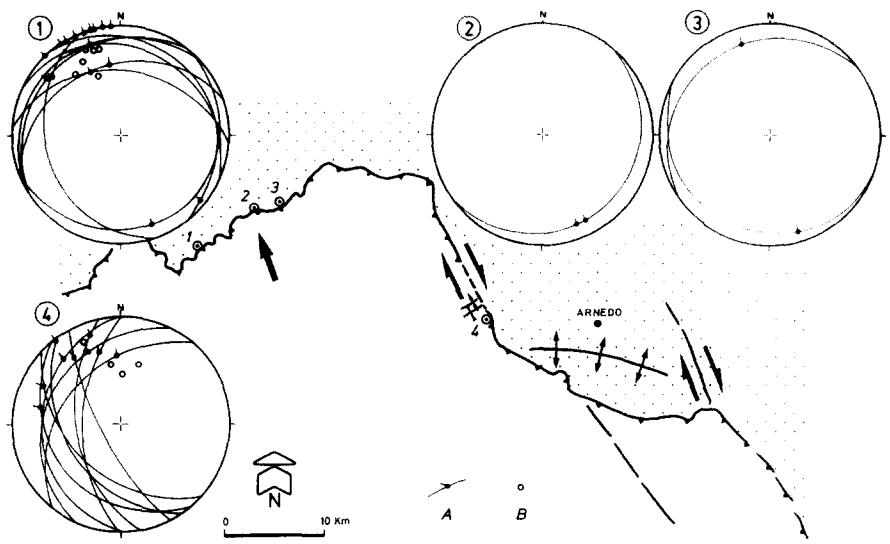

Fig. 4. Kinematic indicators of the transport direction, observed in four outcrops on or close to the thrust surface; A, thrust planes and striations; B, cleavage poles. Arrows indicate the main component of relative displacement on each ramp (according to the kinematic data) resulting in a general transport to the NNW. In sites 1 and 3, an apparent normal movement results from the local NNW dip of the thrust surface.

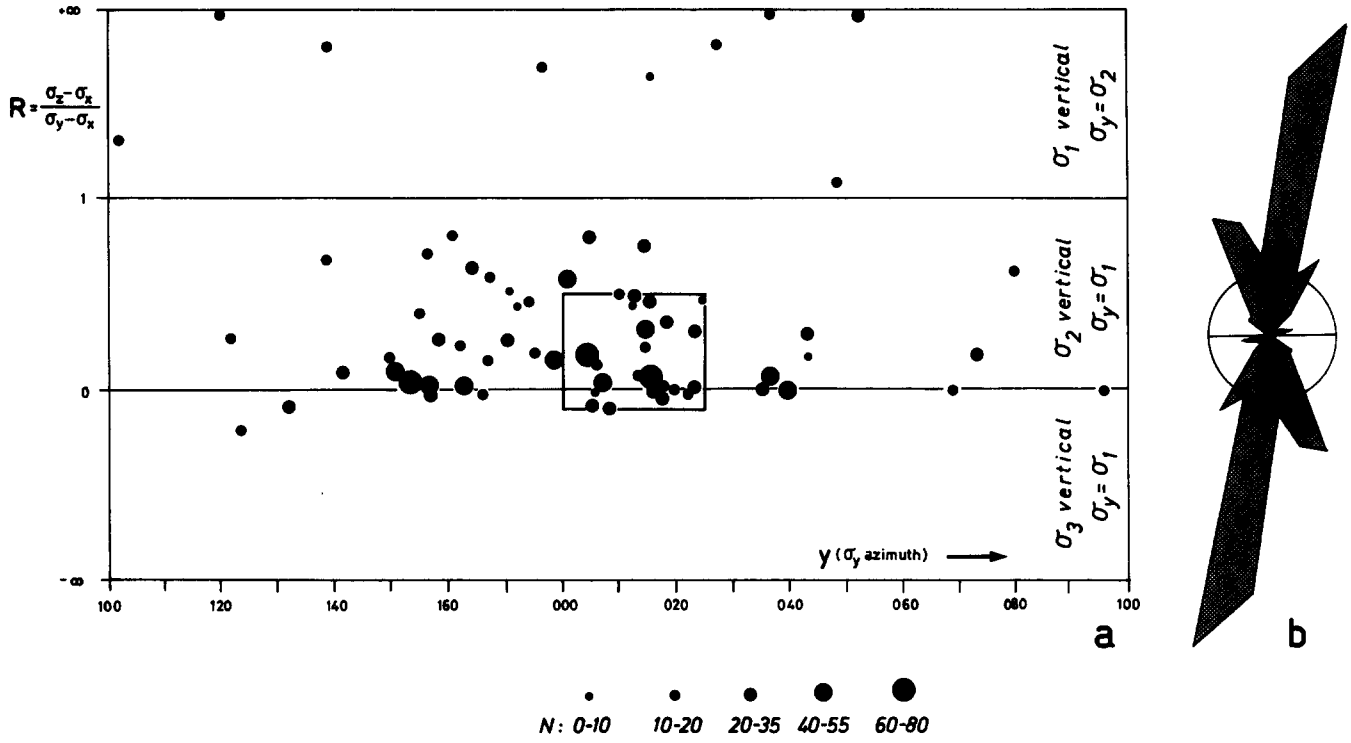

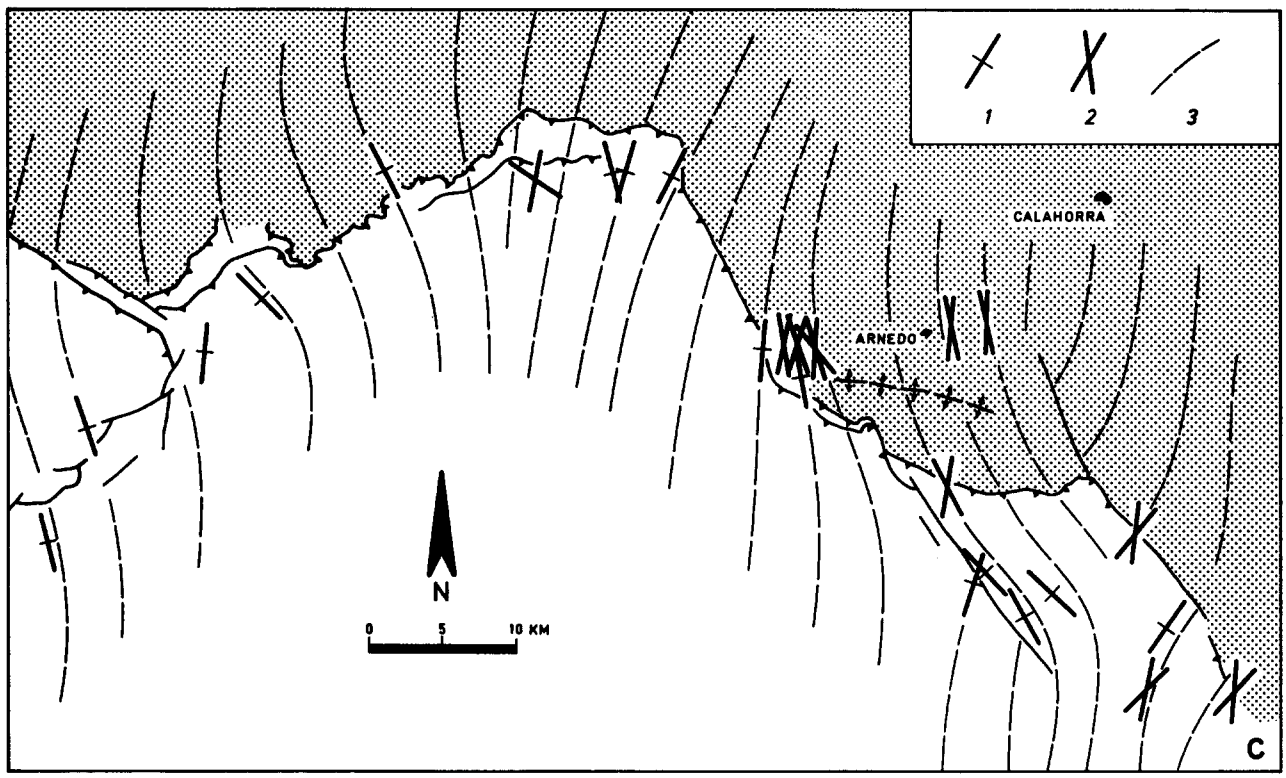

Fig. 5.(a) Synoptic y–R diagram showing all the deviatoric stress tensors inferred from the analysis of fault samples in the whole studied region. N: number of faults defining each tensor. The central rectangle indicates the parameters attributed to the primary or external stress field. (b) Rose diagram of aximuths of horizontal σ_1 axes, weighted according to the number of faults explained by each stress tensor; radius = 5% of data for classes of 10°. (c) Reconstruction of the regional compressional stress field; 1, horizontal stress directions in each mesostructural site; 2, σ_1 directions in sites where several compressional stress tensors were inferred; 3, hypothetic σ_1 trajectories.

expected striations for the standard azimuths of the ramp (155°) and the σ_1 axis (012°). This represents an angle (λ) of 37° between both azimuths. The other diagrams correspond to λ values of 30° and 50°, respectively. In every case three different curves have been drawn for three possible dips of the ramp: 20°, 30° and 40°. It can be seen that the calculated striation pitches tend to be small and positive; this implies a right-

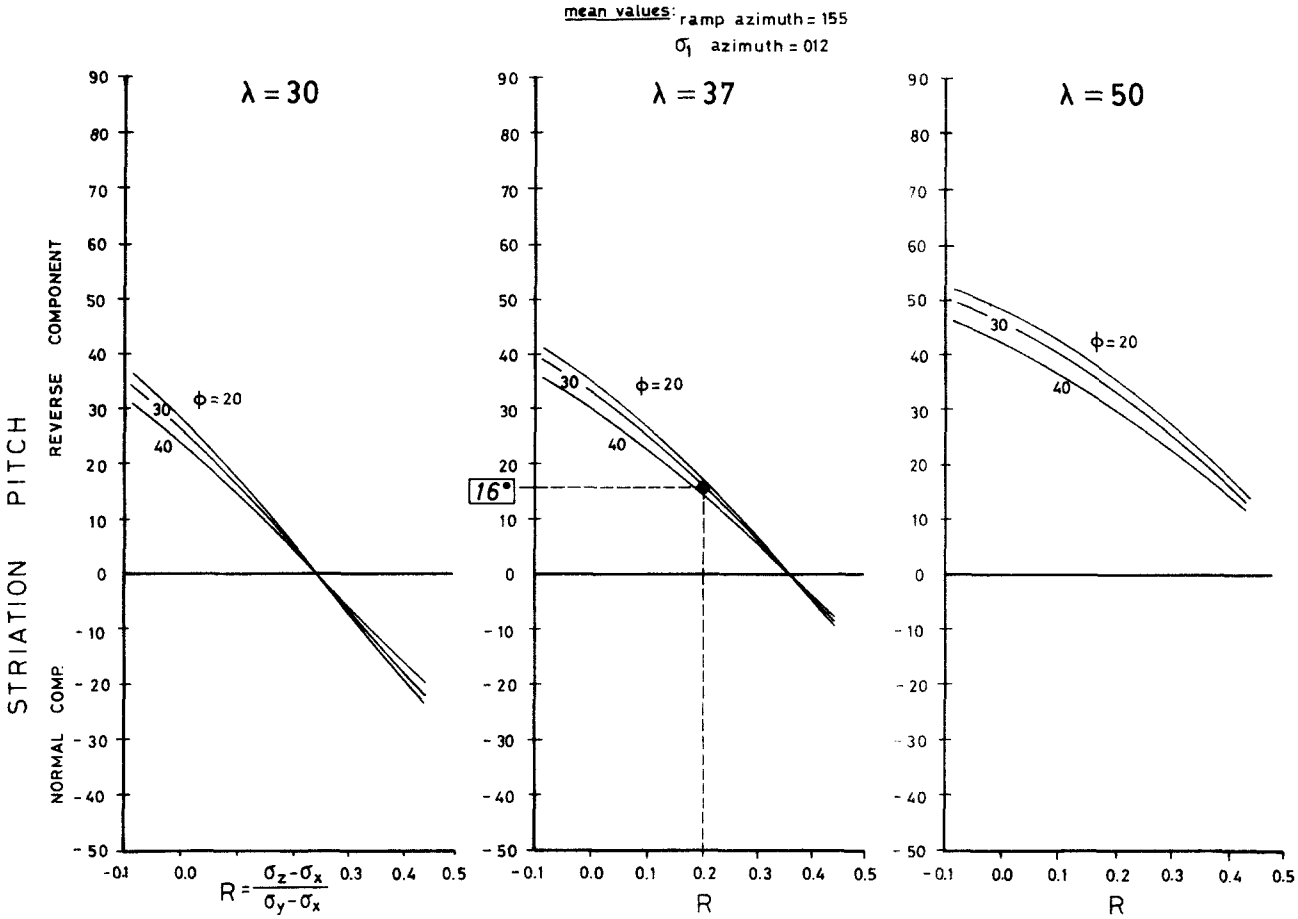

Fig. 6. Calculations of the theoretical pitch of the displacement vector on the eastern ramp of the Cameros Thrust, made by applying Bott's equation to the probable range of values of stress field and ramp orientation. λ, horizontal angle between σ_1 azimuth and ramp strike; ϕ, ramp dip. For the most reliable average values (ramp oriented 155°/30°W, horizontal σ_1 trending 012°, $R = 0.2$) the predicted striation pitch is 16°.

lateral strike-slip movement with a small reverse component, which shows general agreement with field information.

In order to obtain a value for the pitch of the slip vector we can constrain the calculation using the most reliable values of ramp orientation (155°/30°W) and the average stress parameters (012°, horizontal σ_1 axis; $R = 0.2$). In such conditions Bott's equation predicts a pitch of 16° (see the black circle on the central diagram of Fig. 6), which represents a slip vector oriented towards 350° and plunging 8°S. In order to check if the predicted vector agrees with our actual data both components (trend and plunge) must be considered separately because the data needed for their calculation come from independent sources. Firstly, the 350° azimuth should be compared with the 340–345° direction of displacement calculated from kinematic indicators; the agreement is good. Secondly, the predicted plunge of 8° also approaches that deduced from the ratio between the vertical and horizontal offsets measured on the structural cross-section of Fig. 2, which runs approximately parallel to the transport direction. This ratio gives an angle of 12° which is only slightly greater than the calculated value. So we can conclude that the inferred movement on the eastern ramp can be adequately explained under the regional stress field according to Bott's equation.

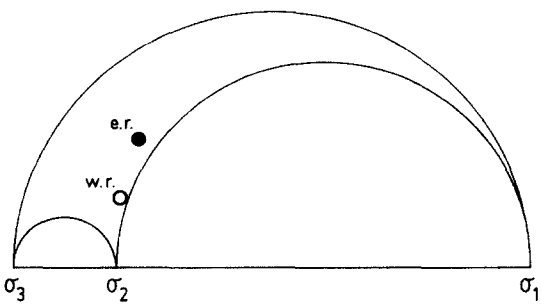

Fig. 7. Mohr diagram of the mean regional deviatoric stress with plotting of planes corresponding to the average orientations of the eastern (e.r.) and western (w.r.) ramps.

On the contrary, the frontal ramp (060°/13°S) could not move purely as a reverse fault since application of Bott's equation to this plane, considering a σ_1 direction between 000° and 025°, would only produce such movement for $R \approx -15$, which is not compatible with our data. This is not a surprising result. If the Cameros Massif actually moved as a rigid block following a fixed transport direction, both ramps underwent simultaneous, not independent slip. In such conditions the general rule is that only one of the two movements can be determined directly by the stress field, whereas the other one should be a 'guided movement' (in the sense of Etchecopar

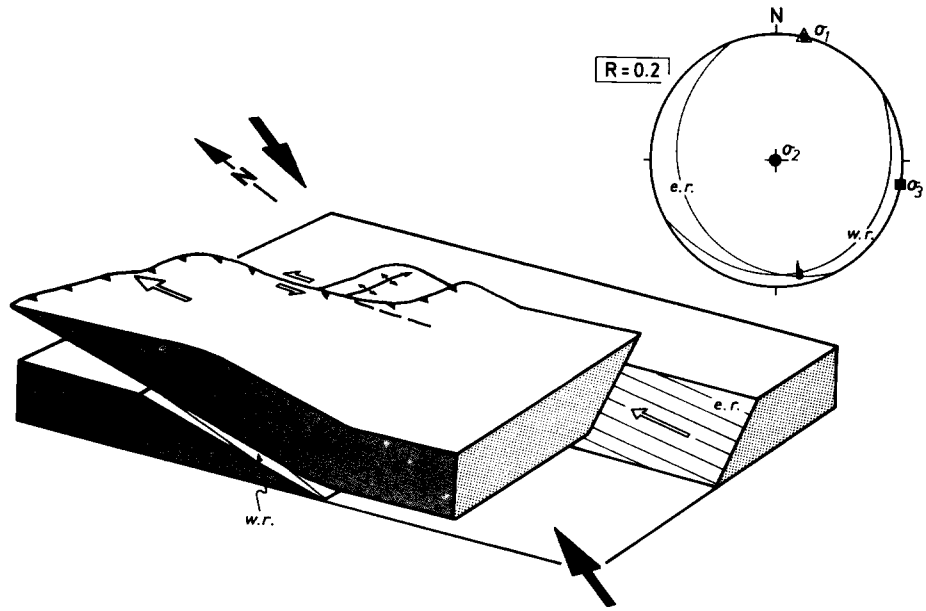

Fig. 8. Kinematic–dynamic model proposed for the Cameros Thrust movement, including the regional stress field and the resulting displacements on the two main ramps. The movement on the eastern ramp (e.r.) is controlled directly by regional stress, whereas that on the western ramp (w.r.) is a 'guided movement' induced by the rigid behaviour of the Cameros block. Stereoplot: Schmidt net, lower-hemisphere.

1984). In our case, it seems to be clear that the stress-controlled slip occurred on the eastern, nearly lateral ramp, and the guided slip occurred on the western, nearly frontal ramp.

The application of the Mohr–Coulomb failure criterion gives further support to this model. If we represent the planes of both ramps on a Mohr diagram (Fig. 6b) we find that the orientation of the eastern ramp is more adequate for slipping under the calculated stress field than the western one.

CONCLUSIONS

Intraplate thrusting of the Cameros Massif over the Tertiary Ebro Basin during the Oligocene to Middle Miocene represents a case of tectonic inversion with respect to the Upper Jurassic–Lower Cretaceous episode of subsidence of the Cameros Basin. Listric normal faults that controlled the development of the basin moved with a reverse component during the Alpine Orogeny, using the clay and gypsum beds of the Keuper as a detachment level. The small amplitude of internal deformations in the sheet relative to the throw of the thrust suggests a relatively rigid behaviour of the Cameros Massif, which may be attributed to the large thickness of Mesozoic deposits (about 5000 m) and the hardening caused by incipient metamorphism.

The direction and sense of displacement, as inferred from kinematic indicators, was 340–345°. This implies that the main normal faults of the Cretaceous basin, oriented 155°/30°W, underwent right-lateral movement with a small reverse component, being nearly a lateral ramp of the thrust. At the same time, another shallower dipping fault plane, striking 060° and bordering the basin to the north-west, moved as frontal ramp (near pure reverse slip) (Fig. 7).

This kinematic scheme may be explained under the regional stress field propagated through the Iberian plate from its convergent northern boundary. Palaeostress analysis from fault striation data allows us to characterize the primary or external stress field as a 000–025° horizontal compression with stress ratio $R = (\sigma_z-\sigma_x)/(\sigma_y-\sigma_x)$ comprised between 0.5 and −0.2 (although it is deflected around major faults). Introducing these parameters into Bott's equation, the predicted slip vector on the SSE ramp shows a mainly right-lateral strike-slip component with a small reverse one (average pitch of 16°). This agrees with the inferred 340–345° azimuth of displacement and the vertical–horizontal offset ratio deduced from deep structural sections. However, the reverse movement on the 060° ramp cannot be explained in the same way and its orientation is not so auspicious as the other for sliding according to the Mohr–Coulomb criterion. Nevertheless, it can be explained as a 'guided movement' induced by the rigid displacement of the Cameros block.

A last reference to the relation between the Cameros and Demanda thrusts is now necessary. As we have said in the introductory section, there exists a convergence component between both massifs, their respective displacement vectors being relatively independent. Our model deals only with the kinematics of the Cameros Thrust, so that any extrapolation to the Demanda Thrust is not justified.

Acknowledgements—We are very grateful to R. J. Lisle for his detailed revision of the manuscript, and to the two reviewers, A. Etchecopar and J. Guimerà, for their useful suggestions. Work leading to this paper has been partially supported by D.G.I.C.Y.T., Spain (project GE091–0924).

REFERENCES

Angelier, J. & Mechler, P. 1977. Sur une méthode graphique de recherche des contraintes principales également utilisable en tectonique et en séismologie: la méthode des dièdres droits. *Bull. Soc. géol. Fr.* **19**, 1309–1318.

Bott, M. H. P. 1959. The mechanics of oblique slip faulting. *Geol. Mag.* **96**, 109–117.

Casas-Sainz, A. 1990. El frente norte de las Sierras de Cameros. Estructuras cabalgantes y campo de esfuerzos. Unpublished Doct. thesis, University of Zaragoza.

Casas, A. M., Simón, J. L. & Serón, F. J. In press. Stress deflection in a tectonic compressional field: a model for the north-western Iberian Chain (Spain). *J. geophys. Res.*

Etchecopar, A. 1984. Etude des états de contraintes en tectonique cassante et simulations de déformations plastiques (approche mathématique). Unpublished Doct. Thesis, U.S.T.L. Montpellier.

Etchecopar, A., Vasseur, G. & Daignières, M. 1981. An inverse problem in microtectonics for the determination of stress tensors from fault striation analysis. *J. Struct. Geol.* **3**, 51–65.

Gracia, P. J. & Simón-Gómez, J. L. 1986. El campo de fallas miocenas de la Bardena Negra (provs. de Navarra y Zaragoza). *Bol. Geol. y Min.* **97**, 693–703.

Guimerà, J. 1984. Palaeogene evolution of deformation in the northeastern Iberian Peninsula. *Geol. Mag.* **121**, 413–420.

Guimerà, J. 1988. Estudi estructural de l'enllaç entre la Serralada Ibèrica i la Serralada Costanera Catalana. Unpublished Doct. thesis, University of Barcelona.

Guimerà, J. & Alvaro, M. 1990. Structure et évolution de la compression alpine dans la Chaîne côtière catalane (Espagne). *Bull. Soc. géol. Fr.* **6**, 339–348.

Guiraud, M. & Séguret, M. 1984. Releasing solitary overstep model for the Late Jurassic–Early Cretaceous (Wealden) Soria strike-slip basin (North Spain). In: *Strike-slip Deformation, Basin Formation and Sedimentation* (edited by Biddle, K. T. & Christie-Blick, N.). *Spec. Publ. Soc. econ. Palaeont. Miner.* **37**, 159–175.

Ramírez, J. I., Olivé, A., Alvaro, M. & Hernández, A. In press. Mapa geológico de España 1:50,000, Hoja No. 241 (Anguiano). ITGE, Madrid.

Simón-Gómez, J. L. 1986. Analysis of a gradual change in stress regime (example from the eastern Iberian Chain, Spain). *Tectonophysics* **124**, 37–53.

Tischer, G. 1966. El delta Weáldico de las Montañas Ibéricas Occidentales y sus enlaces tectónicos. *Not. y com. delIGME* **81**, 53–78.

Xiaohan, L. 1983. Perturbations de contraintes liées aux structures cassantes dans les calcaires fins du Languedoc. Observations et simulations mathématiques. Unpublished III Cycle thesis, U.S.T.L. Montpellier.